Iranian Journal of Geophysics, Vol 17 No 3, 2023, Page 1 – 12 (Research Article)
DOI: 10.30499/IJG.2023.360389.1455

Three-dimensional seismic response of earth dams subjected to spatially varying earthquake ground motion

Amir Ghalyanchi Langroudi [1], Mohammad Davoodi [2*], Mohammad Kazem Jafari [3] and Masoud Nekooei [4]

[1] *Ph.D. Candidate, Department of Civil Engineering, Science and Research Branch, Islamic Azad University, Tehran, Iran*
[2] *Associate Professor, Geotechnical Engineering Research Center, International Institute of Earthquake Engineering and Seismology (IIEES), Tehran, Iran*
[3] *Professor, International Institute of Earthquake Engineering and Seismology, Tehran, Iran*
[4] *Assistant Professor, Department of Structural Engineering, Science and Research Branch, Islamic Azad University, Tehran, Iran*

(Received: 13 September 2022, Accepted: 28 January 2023)

Abstract
For extended structure, the seismic load has a spatiotemporal variation that simultaneously changes with time and space. The incorporation of the seismic wave spatial random variability effect is especially important when large structures such as long bridges, dams, and large buildings are analyzed. The effect of spatially varying earthquake ground motion (SVEGM) on the seismic response of earth dams is analyzed in this paper. To this end, a parametric study is conducted to investigate the effects of length to height ratio (L/H) on the 3D seismic response of the studied dams. Ground motions, consistent with the three-directional lagged coherency model, are generated at different discretized cells at the base of the dam. The dams are assumed to sit on trapezoidal and V-shaped canyons and vibrate in all three directions, upstream-downstream, vertical, and longitudinal. The average coherency of different frequencies is calculated and used for the generation of SVEGM. The time histories are simulated using a spectral representation-based method. The separation distance between the cells is determined in such a way that 90% of correlation between seismic input motions can be captured. For each case of L/H ratio, a numerical model of the dam and its foundation is constructed using the finite difference numerical method. The 3D seismic behavior of the earth dams is evaluated under the artificially generated three-directional components of SVEGM. Generally, it is concluded that with increasing L/H ratio, at the midpoint of the dam crest, the difference between maximum of acceleration values obtained by applying uniform and SVEGM excitations decreases. In all cases of analyses, SVEGM has decreasing effect on the vertical displacement of dam crest.

Keywords: SVEGM, earth dam, coherency model, finite-difference numerical method, dynamic analysis

*Corresponding author: m-davood@iiees.ac.ir

1 Introduction

The spatially varying earthquake ground motion (SVEGM) is a phenomenon in which the ground motion at the base of the extended structures (such as long bridges, tunnels, pipelines, dams, large foundations, among others) differs; hence, the seismic action cannot be defined using the motion at a single point (Efthymiou, 2019).

In most research studies, the spatial variation of ground motion comprises the following attributes: the wave passage effect that arises from the differences in the arrival time of seismic waves at different stations and incoherence effect arising from reflection and refraction of the seismic waves along the path from the source to the site. The incoherence effect can be defined by a coherence function which accounts for the degree of correlation of the earthquake time histories exciting adjacent support in the frequency domain. Local site effects caused by the differences in the local soil conditions at various locations affect the amplitude and frequency content of the seismic waves. Complex topographic effects are due to the scattering of seismic waves caused by irregular topography. SVEGM has a considerable effect on extended structures or multi-support structures such as dams, bridges, pipelines, nuclear power plants, among others.

The dynamic response of earth dams subjected to SVEGM has caught the attention of many researchers. Chen and Harichandran (2001) investigated the stochastic response of the Santa Felicia earth dam subjected to SVEGM characterized by wave propagation and incoherence effects. The investigation suggested that the higher the loss of coherency, the more significant the increase of the maximum shear stress in the stiff gravel of the stream bed. Uniform ground motions yielded slightly conservative responses in terms of displacement, maximum shear strain and maximum shear stresses within the core of the dam. Haroun and Abdel-Hafiz (1987) analyzed the effect of differential ground motions on the response of an earth dam. The earth dam was modelled as a two dimensional shear beam. It was found, in the case of earth dams with relatively large length-to-height ratios, the maximum response at the mid-point of the dam was produced by SVEGM input analysis. Dakulas and Hashmi (1991) derived mathematical solutions for the lateral response of earth and rockfill dams subjected to obliquely incident harmonic SH-waves in semi-cylindrical and rectangular canyons. It was found that the dam response can be sensitive to the assumed form of the canyon rock flexibility, and that the assumption of a rigid base yielded conservative results. Seismic responses of Marun and Masjed-Soleyman embankment dams subjected to SVEGM excitation were determined by Davoodi and Sadreddini (2010), Sadreddini and Davoodi (2010), Davoodi et al. (2013) and Sadrolddini et al. (2013) using 2D and 3D numerical finite difference approaches. It was found that applying SVEGM resulted in a reduction of acceleration values within the core of the dam.

The necessity of this study is that it explores the effect of SVEGM and canyon geometry on the dynamic behavior of earth dam. In this paper, typical models that can capture essential features of the earthquake behaviors of earth dams located at trapezoidal and V-shaped canyons under uniform and SVEGM input motions are investigated. The response of 3D seismic analysis of earth dams is systemically analyzed and compared. The SVEGM is generated using the three-directional coherency model developed by Liu and Hong (2016).

2 Generation of three-component SVEGM

For the numerical analysis, the simulation procedure used in Liu and Hong (2015) is followed. The power spectral matrix for n_R sites, $\mathbf{S}(f)$, which has a dimension of

$3n_R \times 3n_R$, is defined by four sub-matrices, each with the dimension of $n_R \times n_R$:

$$S(f)=\begin{bmatrix} S_{11}(f) & S_{21}(f) & S_{31}(f) \\ S_{21}(f) & S_{22}(f) & S_{23}(f) \\ S_{31}(f) & S_{32}(f) & S_{33}(f) \end{bmatrix} \quad (1)$$

where the elements of the $S_{pq(f)}$ for p and q = 1, 2 or 3 are given by:

$$S_{pq,jk}(f)=S(f)\bar{\gamma}_{pq,jk}(\Delta_{jk}, f), \quad \text{j,k} = 1, \dots, n_R \quad (2)$$

For the simulation, if the spectral representation method (SRM) with the Cholesky decomposition is adopted, the three-directional ground motion at the n_R sites is given by:

$$u(t)=\sum_{i=1}^{N}\sqrt{2 f_\Delta}\left[L(f_i)\otimes C_i\right] \quad (3)$$

where $L(f_i)$ denotes the lower triangular matrix obtained from the Cholesky decomposition of $S(f)$. The operator $\otimes$ is defined as the dot product of the k-th row in C_i to k-th row of $L(f_i)$. C_i denotes a matrix whose elements $C_{jk,i}$ are given by:

$$C_{jk,i} = \cos\left(2\pi f_i + \tan^{-1}\left[\frac{\Im(l_{jk}(f_i))}{\Re(l_{jk}(f_i))}\right] + \phi_{k,i}\right), \quad \text{j,k} = 1, 2, \dots, 3n_R \quad (4)$$

$\Im(\cdot)$ and $\Re(\cdot)$ represent the imaginary and real part of their arguments, respectively. $L_{jk}(f_i)$ is the element of $L(f_i)$. ϕ_{ki} is independent and identically distributed uniform variable between 0 to 2π.

The lagged coherency used in this study is:

$$\left|\bar{\gamma}_{12,jj}(0, f)\right| = c_0 - c_1 f \quad (5)$$

$$\left|\bar{\gamma}_{pp,jk}(\Delta, f)\right| = A\exp\left(-\frac{2\Delta}{\alpha_0\theta(f)}(1-A+\alpha_0 A)\right) + (1-A)\exp\left(-\frac{2\Delta}{\theta(f)}(1-A+\alpha_0 A)\right),$$

$$\theta(f)=k\left[1+\left(f/f_0\right)^b\right]^{-1/2} \quad (6)$$

where c_0, c_1, A, α_0, k, f_0 and b are the model parameters.

The acceleration time history and related spectral amplitude of generated three-component SVEGM at cell 1 is shown in Figure. 1. These generated ground motions are used as input motions in uniform case.

3 Cases of analyses

According to the previous studies, the key factors influencing the dynamic response of an earth dam to seismic loading are the effects of narrow canyon geometry, the dynamic properties of the dam materials, and the nature of the input motions. In this paper, the effects of different canyon geometries including V-shaped canyons and trapezoidal canyons on the dynamic responses of earth dams are studied. The shape ratio L/H (ratio of crest length to the height) of studied dams are 2, 4 and 5. The cases of dynamic analyses are presented in Table 1.

Table 1. Cases of dynamic analyses.

	Trapezoidal canyon			V-shaped canyon		
	Case 1 $\frac{L}{H}=2$	**Case 2** $\frac{L}{H}=4$	**Case 3** $\frac{L}{H}=5$	**Case 4** $\frac{L}{H}=2$	**Case 5** $\frac{L}{H}=4$	**Case 6** $\frac{L}{H}=5$
Length	$L=200$	$L=400$	$L=500$	$L=200$	$L=400$	$L=500$
Height	$H=100$	$H=100$	$H=100$	$H=100$	$H=100$	$H=100$
Foundation size	600×300	600×500	600×600	600×300	600×500	600×600

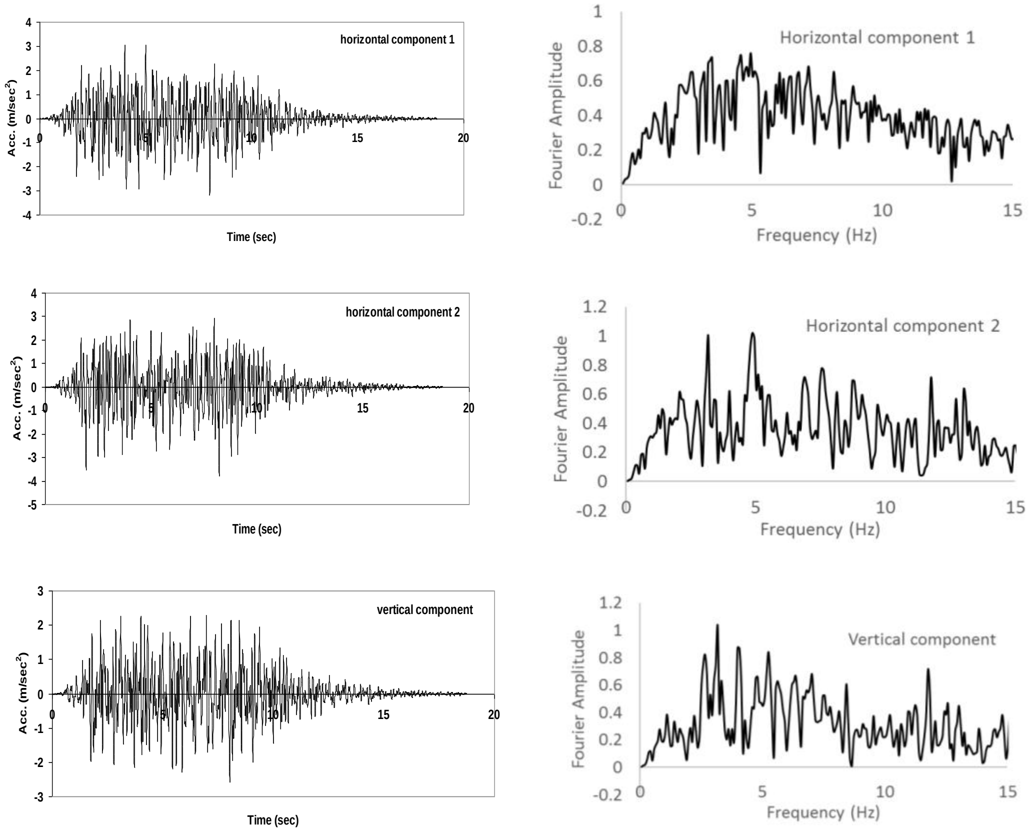

(a) (b)

Figure 1. (a) Three-component generated motions at cell 1. (b) Fourier amplitude of generated seismic motions.

To capture the small scale of the earthquake spatial fluctuation, we can calculate separation distance between cells based on the correlation of 90%. Using the Luco and Wong coherency model (Luco and Wang, 1986) and predominant frequency of the El Centro NS earthquake $\omega = 11\frac{\text{rad}}{\text{sec}}$, we have:

$$d = \frac{\sqrt{-ln|0.9|}}{2.5\times10^{-4}\times11} = 118.03\,m \tag{7}$$

$$\gamma = \exp\left|-(\alpha d\omega)^2\right|$$

where α is coherency drop parameter, γ is the coherency and d is separation distance of stations.

Luco and Wong (1986) proposed that values of α approximately vary from 2×10^{-4} to $3\times10^{-4}\,\frac{s}{m}$.

According to Table 1 and the calculated separation distance of stations, the numbers of the sections for applying SVEGM at the three cases are:

$$\text{Case 1} \begin{cases} n_x = \frac{600}{100} = 6 \\ n_y = \frac{300}{100} = 3 \end{cases} \tag{7}$$

$$\text{Case 2} \begin{cases} n_x = \frac{600}{100} = 6 \\ n_y = \frac{500}{100} = 5 \end{cases} \tag{8}$$

$$\text{Case 3} \begin{cases} n_x = \frac{600}{100} = 6 \\ n_y = \frac{600}{100} = 6 \end{cases} \tag{9}$$

4 Finite difference models

Numerical analyses are conducted using the finite difference program FLAC3D (Itasca Consulting Group, 2002), based on a continuum finite difference discretization using the Langrangian approach.

As mentioned, the effects of different canyon geometries–V-shaped canyons and trapezoidal canyons– on the dynamic responses of earth dams are studied in this paper. The dam embankment consists of a

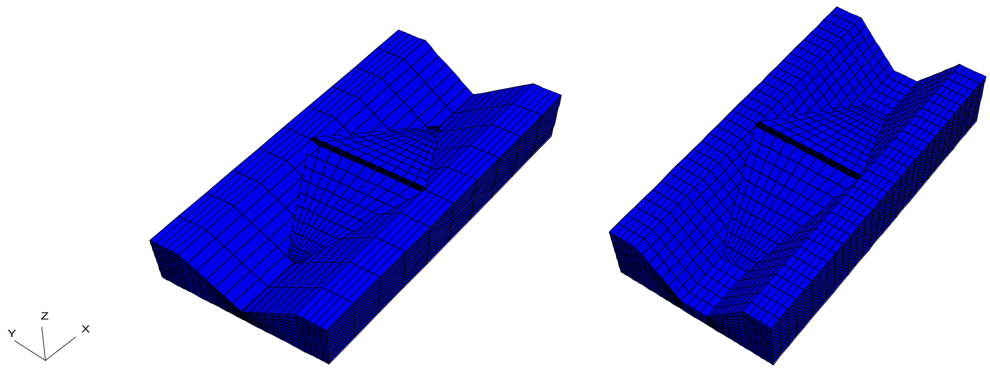

(a) (b)

Figure 2. Three-dimensional finite-difference numerical models. (a) Case 4 for V-shaped canyon. (b) Case 1 for trapezoidal canyon.

Table 2. Material properties.

Section	γ (kN/m^3)	E ×10^6 (kN/m^2)	C (kPa)	ν	ϕ
Core	21.5	0.6	38	0.4	25
Embankment US	20	1.5	-	0.38	39
Embankment DS	20	1.5	-	0.38	35
Foundation	24	12	70	0.31	40

central impervious core and previous shell upstream and downstream. Figure. 2. shows the finite-difference numerical models.

In the current paper, the material of embankments behaves according to the elastic-perfectly plastic Mohr-Coulomb model, and material of foundation and valleys behaves according to the elastic model.

Table 2 summarizes the material properties selected for dynamic analyses of the earth dams. The properties of the dam materials are selected from Sadreddini (2012).

Some of the most important factors that should be considered when preparing a FLAC dynamic model are: (1) seismic inputs; (2) dependence of soil stiffness on confining pressure; (3) element size; (4) boundary conditions. Generally, the shear stiffness G varies with the depth according to Eq. (11):

$$G\left(z/H\right) = G_b \cdot \left(z/H\right)^m \quad (11)$$

where z and H are the vertical distance from the crest of the dam and the height of the dam, respectively. G_b is the shear modulus at the base of the dam and m is the exponent of the stiffness which dictates its variation with depth. In this study, the maximum shear modulus is calculated based on the profile of shear wave velocity (Figure. 3) using the following equation:

$$G_{\max} = \rho V_S^2 \quad (12)$$

The shear wave velocity and frequency control the maximum element size (l_e) according to the Eq. (13):

$$l_e \le \frac{V_s}{6\, f_{\max}} \quad (13)$$

where λ is the wavelength associated with the highest frequency component that contains appreciable energy (Shih et al., 2016).

As shown by the power spectral density of horizontal component 1 at cell 1 (Fig. 4), most of the power (approximately

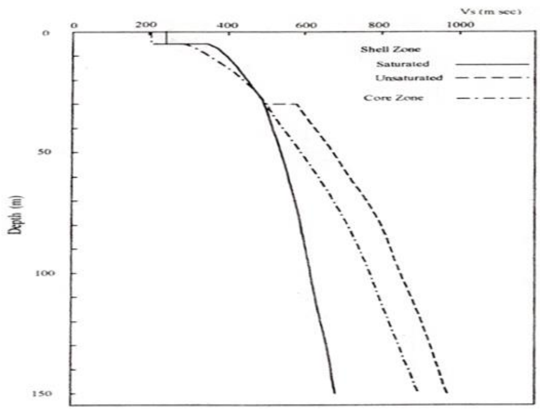

Figure 3. Profile of shear wave velocity used in this study (Nippon Koei Group et al., 1999; Sawada and Takahashi, 1975).

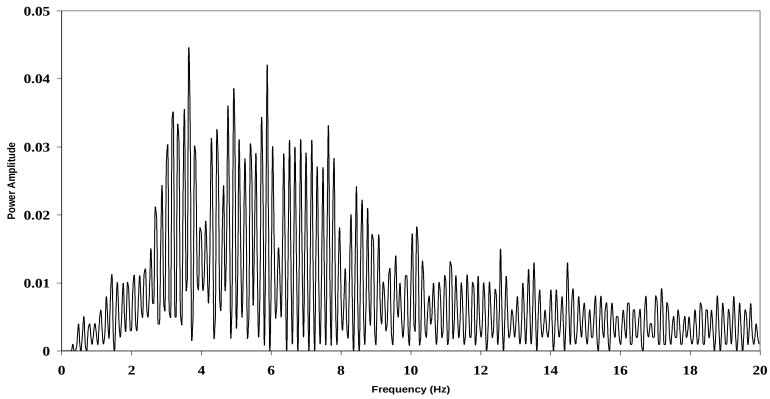

Figure 4. Power spectral density of horizontal component 1 at cell 1.

93.33%) is made up of components of frequency 15 Hz or lower. Therefore, it can be interpreted that by filtering the velocity input motion with a 15 Hz low-pass filter, less than 6.67% of the power is lost.

In order to accurate representation of wave transmission through the model, the largest zone size in the numerical model (Δl) is selected as 4 m. The boundary conditions at the sides of the model must account for the free-field motion that would exist in the absence of the structure (Itasca Consulting Group, 2002).

Boundaries of both sides of the dam are constrained laterally while the bottom boundary of the dam is fixed in both horizontal and vertical directions.

5 Results

The results of dynamic analyses related to the trapezoidal canyon are shown in Figures. 5-11. The results of the case 1 analysis are shown in Figure. (5).

It can be seen from the Figure. 5a that uniform input produces larger values of acceleration than SVEGM input at the middle of dam crest. The maximum Y-acceleration values calculated under SVEGM and uniform excitations are $8\frac{\text{m}}{\text{sec}^2}$ and $6.5\frac{\text{m}}{\text{sec}^2}$, respectively.

Vertical displacement values are higher than those obtained under SVEGM excitation due to uniform excitation. The ratios of crest settlement (S) to the dam height (H) (settlement ratio) calculated are 0.0045% and 0.0037% for the uniform input and SVEGM input analyses, respectively. According to Swaisgood (2003), the permanent settlement of 1% at dam crest can be adopted as an acceptable limit threshold to evaluate dam performance (Figure. 6).

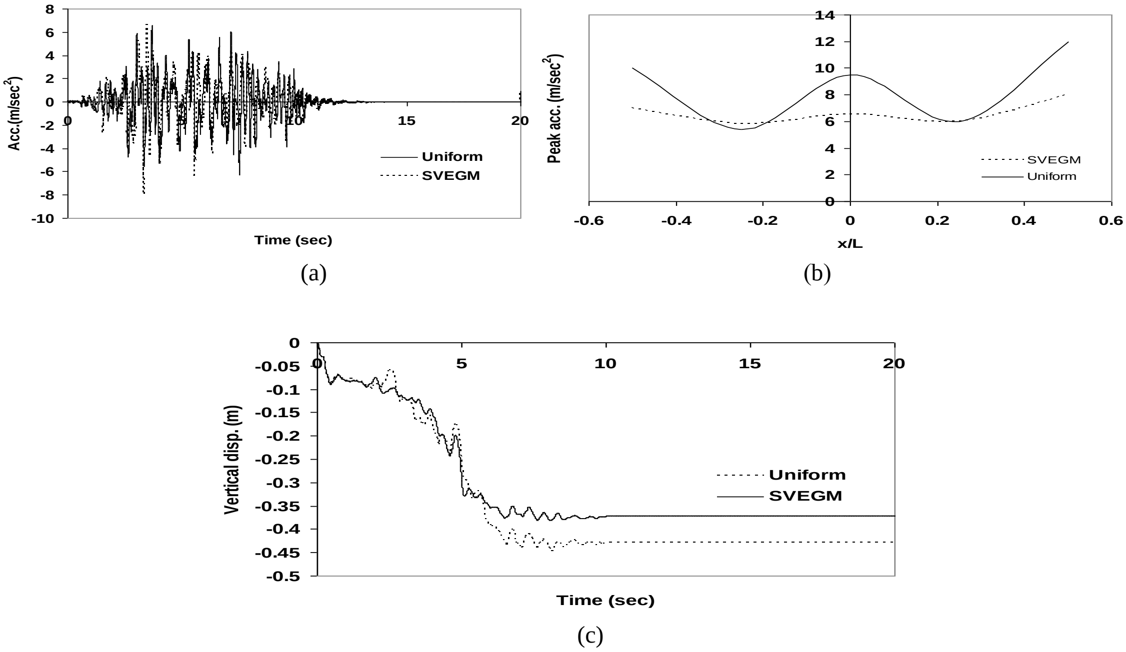

Figure 5. Results of case 1. (a) Peak acceleration along dam crest. (b) Y-acceleration of the midpoint of dam crest. (c) Vertical displacement at the midpoint of the dam crest.

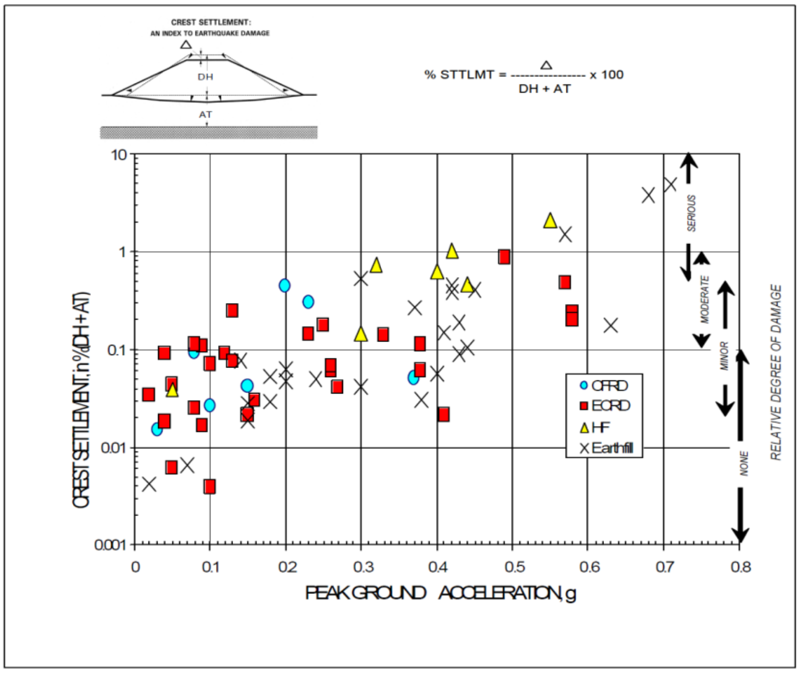

Figure 6. Settlement of embankment dams during an earthquake (Sawada and Takahashi, 1975).

The results of case 2 analysis are shown in Figure. 7.

The values of peak X-accelerations for analyses with uniform and SVEGM input motions are near each other. The maximum Y-acceleration values obtained with uniform and SVEGM excitations are about $7\,\dfrac{\text{m}}{\text{sec}^2}$ and $6\,\dfrac{\text{m}}{\text{sec}^2}$, respectively. The uniform input motion results in larger vertical displacement that reaches 45 cm at the end of excitation. The settlement ratios S/H calculated are 0.0045% and 0.0030% for the uniform input and SVEGM input analyses, respectively.

The results of the case 3 analysis are shown in Figure. 8.

It is observed that at the midpoint of the crest, the peak X-accelerations values subjected to uniform and SVEGM excitations are about $8\frac{\mathrm{m}}{\mathrm{sec}^2}$ and $7.5\frac{\mathrm{m}}{\mathrm{sec}^2}$, respectively. The maximum Y-acceleration values at the midpoint of the crest obtained with uniform and SVEGM excitations are about $6.3\frac{\mathrm{m}}{\mathrm{sec}^2}$ and $6.7\frac{\mathrm{m}}{\mathrm{sec}^2}$, respectively. Regarding Figure. 8c, the vertical displacements at the end of excitation are about 30 cm and 43 cm for uniform and SVEGM excitations, respectively.

The results of dynamic analyses related to V-shaped canyon are shown in Figures. 9-11. Figure. 9 shows the results of the case 4 analysis.

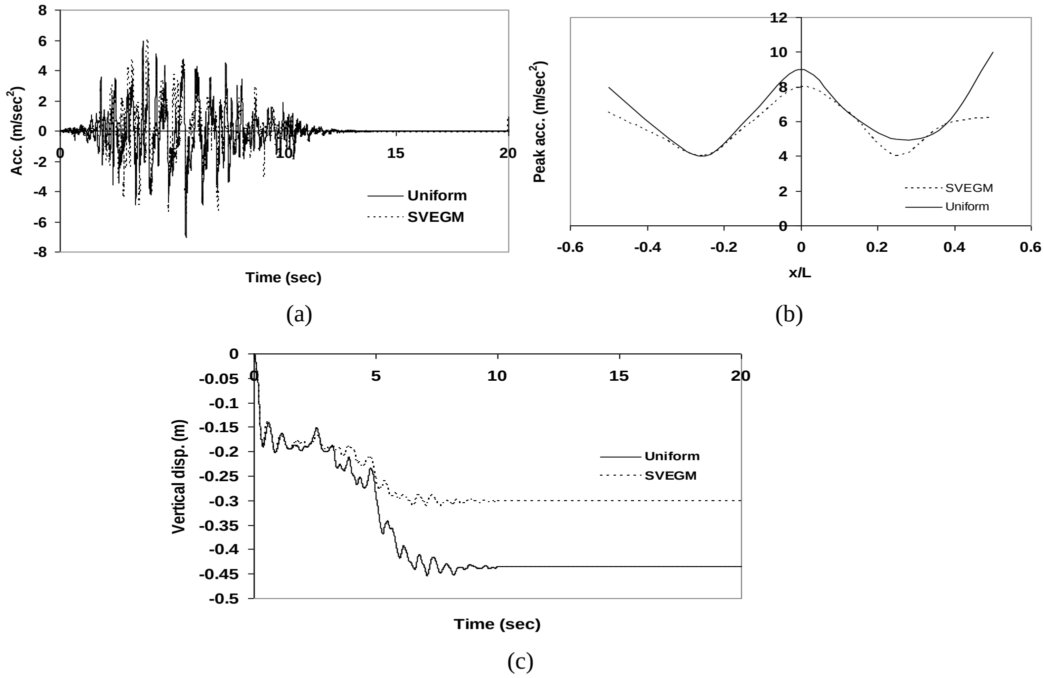

(a) (b) (c)

Figure 7. Results of case 2. (a) Peak acceleration along dam crest. (b) Y-acceleration of the midpoint of dam crest. (c) Vertical displacement midpoint of the dam crest.

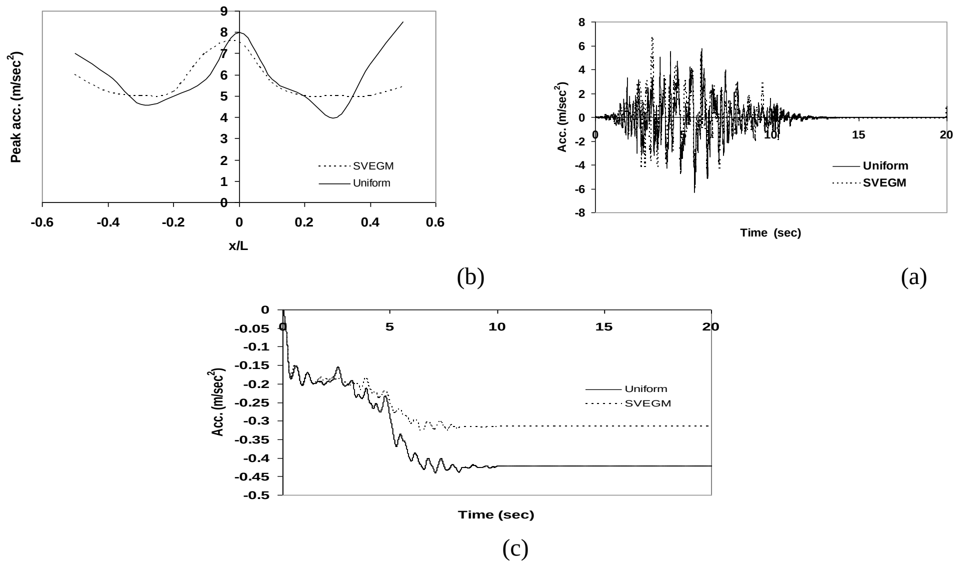

(b) (a) (c)

Figure 8. Results of case 3. (a) Peak acceleration along dam crest. (b) Y-acceleration of the midpoint of dam crest. (c) Vertical displacement midpoint of the dam crest.

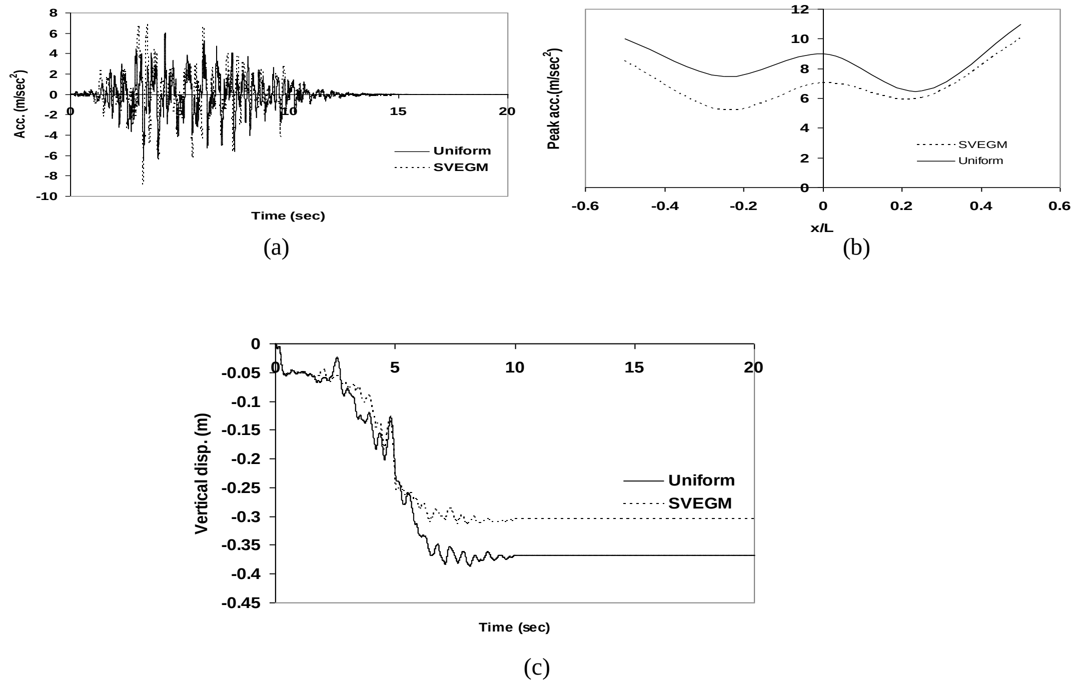

Figure 9. Results of case 4. (a) Peak acceleration along dam crest. (b) Y-acceleration of the midpoint of dam crest. (c) Vertical displacement midpoint of the dam crest.

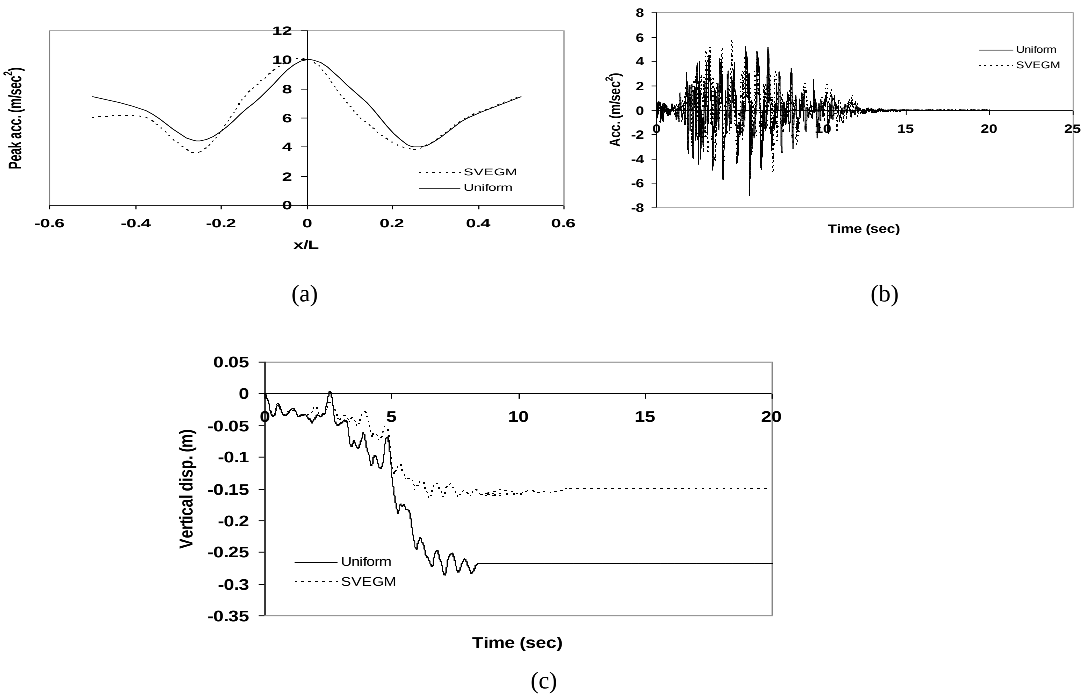

Figure 10. Results of case 5. (a) Peak acceleration along dam crest. (b) Y-acceleration of the midpoint of dam crest. (c) Vertical displacement midpoint of the dam crest.

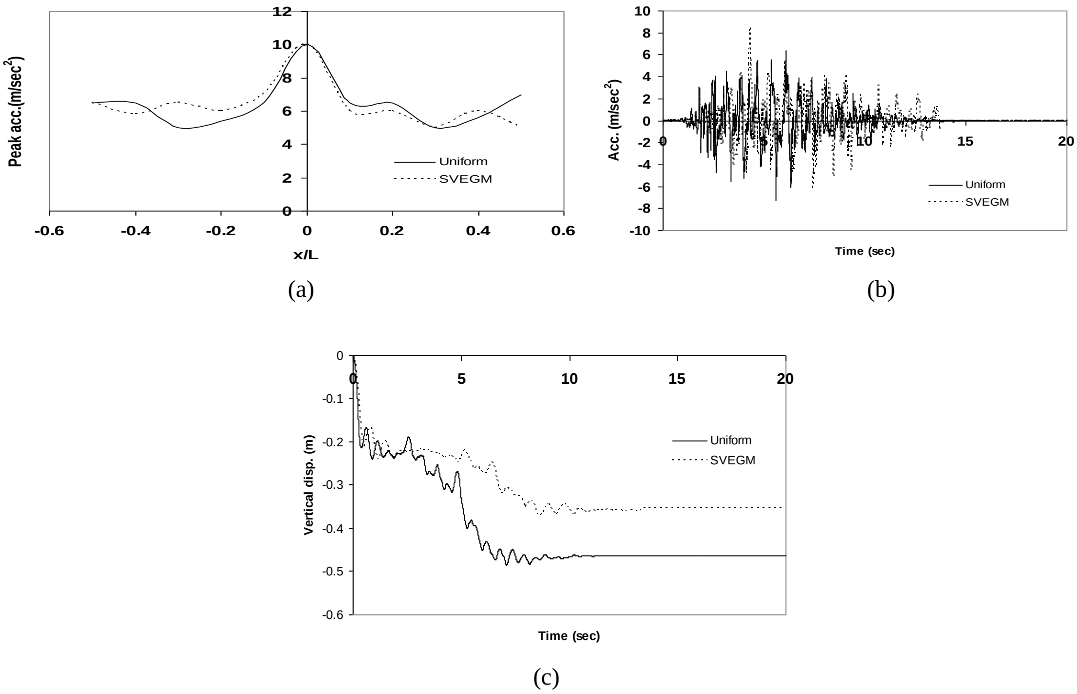

Figure 11. Results of case 6. (a) Peak acceleration along dam crest. (b) Y-acceleration of the midpoint of dam crest. (c) Vertical displacement midpoint of the dam crest.

As can be seen, the pattern of peak acceleration of SVEGM input analysis is similar to the uniform input analysis. The results of uniform input analyses are higher than those obtained from SVEGM input analyses at the whole length of the crest. The maximum Y-acceleration values obtained at the the midpoint of the crest length under uniform and SVEGM excitations are about $6.5\frac{m}{sec^2}$ and $8.8\frac{m}{sec^2}$, respectively. Regarding Figure. 9, the vertical displacements of the midpoint of the crest at the end of excitation are about 37 cm and 30 cm for uniform and SVEGM excitations, respectively.

Figure 10 depicts the results of case 5. As can be seen from Figure. 10a, the results of uniform input and SVEGM input analyses are near each other. Figure. 10b shows the Y-acceleration time histories of the midpoint of the dam crest subjected to uniform and SVEGM input motions. It can be observed that the maximum of the Y-acceleration values obtained under uniform and SVEGM excitations are about $7\frac{m}{sec^2}$ and $5.8\frac{m}{sec^2}$, respectively. Regarding Figure. 10c, the vertical displacements at the end of excitation are about 27 cm and 15 cm for uniform and SVEGM excitations, respectively. Figure. 11 shows the results of the case 6 analysis.

It can be said that the maximum of peak accelerations (about $10\frac{m}{sec^2}$) occurs at the midpoint of the crest in both uniform and SVEGM input analyses. It can be observed that the maximum of the Y-acceleration values obtained with uniform and SVEGM excitations are about $7.3\frac{m}{sec^2}$ and $8.5\frac{m}{sec^2}$, respectively. Regarding Figure. 11c, vertical displacement value obtained from uniform input analysis is 28.6% higher than that calculated by SVEGM input analysis.

The maximum of X- and Y-acceleration values at the midpoint of the dam crest are given in Tables 3 and 4, respectively.

Table 3. Maximum X-acceleration values (m/sec^2) at the midpoint of the dam crest.

Cases	uniform	SVEGM
Case 1	9.5	6.5
Case 2	9	8
Case 3	8	7.5
Case 4	9	7
Case 5	10	10
Case 6	10	10

Table 4. Maximum Y-acceleration values (m/sec^2) at the midpoint of the dam crest.

Cases	uniform	SVEGM
Case 1	6.567	8.017
Case 2	7.02	6.064
Case 3	6.331	6.724
Case 4	6.401	8.883
Case 5	7.043	5.77
Case 6	7.313	8.472

6 Conclusions

The discretization of the foundation spatial domain is performed in such a way that 90% of correlation can be captured. According to this, the base of the foundation is discretized to 18, 30, and 36 regions for cases 1, 2, and 3 (also for corresponding cases 4, 5, and 6), respectively.

Generally, for trapiziodal canyon, the peak X-accelerations values calculated by uniform input analysis are higher than those obtained subjected to the SVEGM excitation at the midpoint of the dam crest, in all cases considered.

For V-shaped canyon, the same peak X-accelerations values are obtained in cases $L/H = 4$ and $L/H = 5$ under uniform and SVEGM excitations.

In regard to the peak Y-accelerations results at the midpoint of the dam crest, in all cases except the case with $L/H = 4$, SVEGM has increasing effect.

In all cases of analyses, SVEGM has decreasing effect on the vertical displacement of dam crest.

This study considers numerical dynamic response of earth dam under three components SVEGM while there is no related research available in this regard. Consequently, we cannot compare our results with other studies. We will try to get access to a recorded acceleration time histories and settlement of an instrumented embankment dam in future. Then, we will be able to compare our analysis results with reality. As yet, we couldn't find such information in past strong earthquakes. The authors wish the results of this study would be useful for the future studies.

References

Chen, M. T., and Harichandran, R. S., 2001, Response of an earth dam to spatially varying earthquake ground motion: Journal of Engineering Mechanics, **127**(9), 932-939.

Dakoulas, P., and Hashmi, H., 1991, Response of earth dams in canyons subject to asynchronous base excitation: Proceeding of Second International Conference of Geotechnic, Earthquake Engineering & Soil Dynamics: St. Louis, **II**, 1105-1112.

Davoodi, M., Jafari, M. K., and Sadrolddini, S. M. A., 2013, Effect of multi-support excitation on seismic response of embankment dams: International Journal of Civil Engineering, **11**(1), 19-28.

Davoodi, M., and Sadreddini, A., 2010, Seismic behavior of a large embankment dam under incoherent ground motions: 4th International Conference on Geotechnical Engineering and Soil Mechanics (ICGESM), Tehran, Iran.

Efthymiou, E. A., 2019, The effect of multi-angle spatially variable ground motions on the seismic behaviour of cable-stayed bridges: City, University of London.

Haroun, M. A., and Abdel-Hafiz, E. A., 1987, Seismic response analysis of earth dams under differential ground motion: Bulletin of the Seismological Society of America, **77**, 1514-1529.

Itasca Consulting Group, Inc., 2002, *FLAC3D — Fast Lagrangian Analysis of Continua in Three-Dimensions,* User's manual: Itasca, Minneapolis.

Liu, T., and Hong, H., 2015, Simulation of horizontal ground motions with spatial coherency in two orthogonal horizontal directions: Journal of Earthquake Engineering, **19**(5), 752-769.

Liu, T., and Hong, H., 2016, Assessment of spatial coherency using tri-directional ground motions: Journal of Earthquake Engineering, **20**(5), 773-794.

Luco, J., and Wong, H., 1986, Response of a rigid foundation to a spatially random ground motion: Earthquake Engineering & Structural Dynamics, **14**(6), 891-908.

Nippon Koei Group, Moshanir, Lahmeyer, 1999, Masjed-E-Soleiman HEEP report on dynamic analysis for the Masjed-E-Soleiman dam.

Sadreddini, A., and Davoodi, M., 2010, Response of a rockfill dam to spatially varying earthquake ground motion: 14th European Confrence on Earthquake Engineering, Ohrid, Macedonia.

Sadreddini, S. M. A., 2012, Evaluation of the effect of spatially varying earthquake ground motion on the seismic behavior of earth dams: PhD thesis, Science and Research Branch, Islamic Azad University, Tehran, Iran, 2012.

Sadrolddini, S. M. A., Davoodi, M., and Jafari, M. K., 2013, Effects of different frequency content of multi-support excitations on seismic response of a large embankment dam: Iranian Journal of Science and Technology, Transactions of Civil Engineering, **37**(C2), 243-256.

Sawada, Y., and Takahashi, T., 1975, Study on the material properties and the earthquake behaviors of rockfill dams: Proceeding of 4th Japan Earthquake Engineering Symposium.

Shih, J. Y., Thompson, D., and Zervos, A., 2016, The effect of boundary conditions, model size and damping models in the finite element modelling of a moving load on a track/ground system: Soil Dynamics and Earthquake Engineering, **89**, 12-27.

Swaisgood, J., 2003, Embankment dam deformations caused by earthquakes: Pacific conference on earthquake engineering.